AN ABSTRACT OF THE THESIS OF

Chi-young Lim for the degree of Master of Science in

Electrical and Computer Engineering presented on December 9, 2003.

Title: Design of Compact Folded-Line RF Power Dividers.

Signature redacted for privacy.

Abstract approved: _____

Andreas Weisshaar

Embedded passives in multi-layer media have gained importance for offering an attractive solution to the implementation of off-chip passive components in RF and mixed signal circuits, especially for wireless applications. Among the passive devices, power dividers and combiners are extensively used for a host of applications including balanced mixers, phase shifters, and feed networks in antenna arrays. The Wilkinson power divider is one of most popular types of power dividers, having ideal transmission characteristics at the center frequency and enabling simple realization in planar transmission line technology. For RF and mixed-signal applications, however, the conventional Wilkinson power divider has a prohibitively large component footprint due to its quarter-wavelength line components. To realize practical Wilkinson power dividers for RF applications, more compact designs with smaller footprint size are developed in this thesis.

A more compact layout is obtained by folding the quarter-wavelength sections in the general multi-level, multi-conductor environment. A C-section with a single fold consisting of two coupled lines is introduced as basic building block. The folded-line concept in single- and multi-level configurations is applied to the design of new compact 3dB Wilkinson RF power dividers. Simple closed-form design equations for

compact 3dB Wilkinson RF power dividers with single C-section and two cascaded C-sections are developed. A significant reduction in footprint between 67% and 83% of the conventional design is achieved. Comprehensive electromagnetic simulations with the full-wave planar electromagnetic simulator *Momentum* are performed for several typical compact designs to validate the proposed design methodology. Good agreement with the full-wave simulation results is demonstrated. For further validation, a compact single level 3dB power divider with two cascaded C-sections designed for 2 GHz center frequency has been fabricated. The measured response is found to be in good agreement with the theoretical response and full-wave simulation results.

Design of Compact Folded-Line RF Power Dividers

by

Chi-young Lim

A THESIS

submitted to

Oregon State University

in partial fulfillment of
the requirements for the
degree of

Master of Science

Completed December 9, 2003
Commencement June 2004

TABLE OF CONTENTS

TABLE OF CONTENTS (Continued)

LIST OF FIGURES

LIST OF FIGURES (Continued)

Figure Page

LIST OF TABLES

DESIGN OF COMPACT FOLDED-LINE RF POWER DIVIDERS

1. INTRODUCTION

Passive electronic components and devices such as resistors, capacitors, and inductors, as well as interconnections are common elements in electronic circuits. In radio-frequency (RF) and microwave systems, functional passive blocks including couplers, filters and power dividers or combiners are also frequently used. These passive components typically occupy a large portion of the space in integrated circuits (ICs) or on printed circuit boards (PCBs). As compactness (smaller size and lighter weight) of many electronic products and, in particular, wireless communications products has been increasingly demanded by the market, the reduction in size of passive components has become essential.

Size reduction of passive components can be achieved by integrating or embedding them into the substrate. The substrate might be ceramic, organic, or a laminate used in PCBs or packages for example for multi-chip modules. One advantage of embedded passives over discrete passives is that discrete passives need to be mounted on the surface and occupy a large portion of the surface area. Also, if the number of passive components is large, the cost of conversion to place components in surface-mount technology (SMT) can be considerable. This can be reduced by parallel processing for embedded passives. Another advantage of embedded passives is that surface mount resistors and capacitors or packaged filters, couplers, or power dividers have inherent parasitics caused e.g. by component or package leads. By embedding passives into the substrate, the parasitics can be significantly reduced.

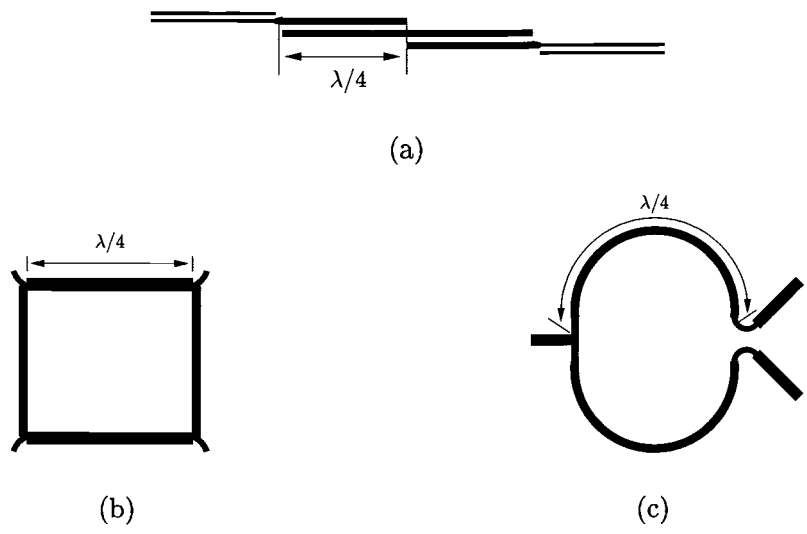

FIGURE 1.1. Various passive components in planar transmission-line technology. (a) coupled-line bandpass filter, (b) branch-line hybrid, (c) Wilkinson power divider.

At microwave frequencies, the theory of passive components such as filters, couplers, and power dividers realized in planar transmission-line technology is quite well established. For the lower frequencies of RF systems (e.g. at 1 GHz), however, the extension of this theory results in large component footprint. Quarter-wavelength lines are often used as basic sections for various passive components in microwave circuits, as illustrated in Figure 1.1. The physical length of these line sections determines the footprint area that will be occupied by the passive component. At a center frequency of 2GHz, for instance, a quarter-wavelength ($\lambda/4$) for an RT-duroid [1] substrate ($\epsilon_r = 2.2$) is approximately 2.5 centimeters. Thus, physical size reduction of the quarter-wavelength line sections is the key for achieving compactness of these passive components when used for RF applications.

Recent increased interest in three-dimensional passive components in radio-frequency integrated circuits (RF IC's) and embedded passives in RF and mixed-

signal modules especially for wireless communication systems demonstrates the importance of the size reduction of passive components. For example, the design of inductors and capacitors for both RF ICs and off-chip multi-layer media has recently been the focus of attention. In particular, embedded passives in multi-layer media have gained importance for offering an attractive solution to the implementation of off-chip passive components in RF and mixed-signal circuits. Design methodologies for new compact components and circuits having small footprint in layered media for RF applications are being developed by a number of people in the field. For example, the analysis and design of multi-layer coupled line filter circuits has recently been reported in [2, 3]. Tripathi *et al.* [4] have reported the analysis and design of a branch-line hybrid using coupled lines. Another example of the use of coupled lines for compact size is in hair-pin resonator filter designs [5]. Furthermore, new compact topologies taking advantage of the 3-D environment in designing passive circuits for integrated circuits have been reported [6].

A more compact layout can be achieved if the conventional transmission lines are folded in a multi-level, multi-conductor environment. For example, the simple C-section described in [7] for application as a fixed passive phase shifter can also be considered as a basic folded-line structure. In particular, the quarter-wavelength line can be very attractive when it is folded as illustrated in Figure 1.2. The folded-line structure can be treated in terms of a set of general coupled lines. The main idea is to replace a straight quarter-wave line section with a folded-line configuration of smaller physical size but with the same electrical characteristics as the straight section at the design frequency. The folded line essentially is a set of coupled lines interconnected at the ends. Thus, the folded-line structure can be designed based on general coupled-line theory and can provide a common approach for the design of

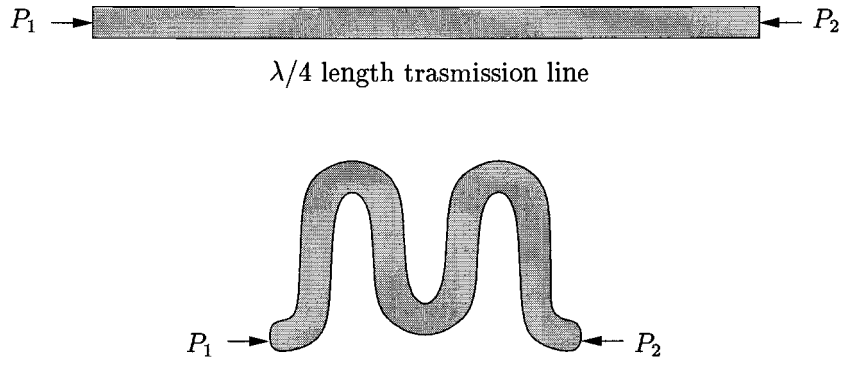

FIGURE 1.2. Illustration of the concept of a folded line.

embedded passive components having significantly reduced footprint size compared to the conventional designs.

Power dividers and combiners are extensively used in microwave frequencies for a host of applications including balanced mixers, phase shifters, and feed networks in antenna arrays. The possible application of the power divider in a QAM (Quadrature Amplitude Modulation) receiver is illustrated in Figure 1.3. The in phase power divider is used to split the RF input signals and to feed the RF ports of the double balanced mixers. The LO (Local Oscillator) signal is fed to the hybrid and split with a 90 deg phase shift between the two outputs before feeding the LO ports of the double-balanced mixers. The two double-balanced mixers provide the IF (Intermediate Frequency) outputs (I and Q) that are equal in amplitude, but inphase quadrature. The mixers multiply the RF and LO signals, and since the quadrature hybrid introduces a 90 deg phase difference, mixer 1 multiplies $cos(\omega_{LO}t)cos(\omega_{RF}t)$, while mixer2 multiplies $sin(\omega_{LO}t)cos(\omega_{RF}t)$.

Another example of an application of the power divider is in feeding networks in antenna arrays. One of the practical ways to improve the overall performance

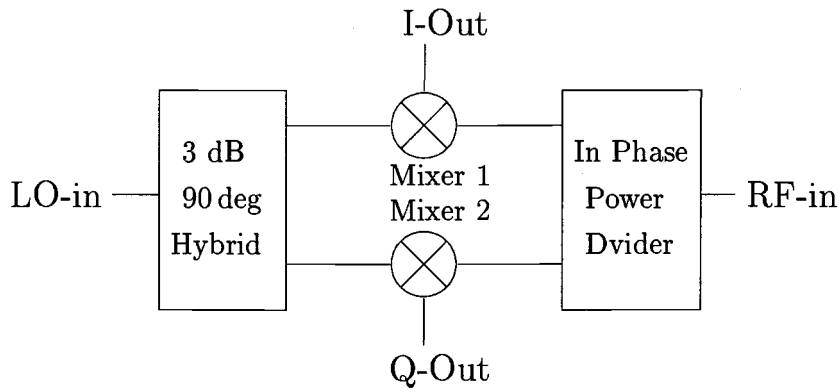

FIGURE 1.3. Application of a power divider in a QAM receiver

of any antenna network is to use multiple antennas phased in such a way so that the total gain of the array increases. The simplest configuration is intended to combine two antennas, each with an impedance of e.g. 50 ohms. If the two antennas were directly connected together in parallel with equal lengths of 50-ohm cables, the resulting impedance at the joined ends would be 25 ohms. If this is connected to another 50 ohm system, it would cause a 'mismatch' in the system. If the characteristic impedance is transformed from 50 ohm to 100 ohm for the two antennas at the joint, the resulting impedance at the joined end would be 50 ohm again. The inphase power combiner can provide such a solution in that it acts like an impedance transformer from 50 ohm to 100 ohm at the joint of the two antennas.

The Wilkinson power divider [8] is particularly attractive because of its ideal inphase transmission characteristics at the center frequency and simple realization in planar transmission-line technology [9]. Unlike the lossless T-junction divider, the Wilkinson power divider can have all ports matched and achieve perfect isolation between two output ports. The conventional design of the two-way Wilkinson power divider consists of two quarter-wave transmission line sections, which give in

a small footprint at higher microwave frequencies. For RF and mixed-signal applications, however, the conventional Wilkinson power divider has a prohibitively large component footprint. To realize the Wilkinson power divider at radio frequencies (RF), more compact designs with smaller footprints are needed. The motivation of this thesis is the minimization of the footprint size of the quarter-wavelength lines, to achieve more compact Wilkinson power divider designs at radio frequencies.

This thesis presents a comprehensive design methodology for single- and multi-conductor level compact folded-line RF power dividers. The compact power dividers are based on the conventional Wilkinson power divider concept combined with folded-line quarter-wavelength sections. The properties of the folded lines are obtained in terms of a network representation of coupled lines. This work is also an extension of the application of the folded-line concept to compact multi-level folded-line RF couplers [10, 11] and compact RF filters [12].

Chapter Two reviews several conventional types of power dividers. The lossless as well as the resistive T-junction power dividers are analyzed and their basic properties are studied. Then, the operation of the conventional Wilkinson power divider is described in more detail. The inherent advantages of the Wilkinson power divider over the T-junction power dividers are also discussed.

Chapter Three presents an analysis of general folded-line structures. This is accomplished by a network representation of the corresponding coupled-line system. As a basic building block, a single C-section, which consists of two coupled lines interconnected at one end, is considered. Also, the scattering matrix of a single level C-section with ideal interconnection is derived. For the realization of this C-section, the effect of the transmission-line interconnection is included and the response of the C-section is tuned to match that of the ideal C-section.

Chapter Four describes a design procedure for single- and multi-level 3 dB power dividers using the folded-line concept. The design of the conventional 3dB Wilkinson power divider is first reviewed. New simple design equations for compact 3dB power dividers for both cases with one C-section and two cascaded C-sections are developed. Based on these design equations, examples of compact 3dB power divider designs are presented for the single- and multi-level cases. Also, other design issues including physical layout geometries and tuning for optimal response are discussed. The full-wave electromagnetic simulator *Momentum* [13] is used for preliminary validation.

Chapter Five addresses implementation issues for the compact single-level folded-line 3 dB power divider fabricated on RT-Duroid material. The implemented circuit is measured with an HP-8722 Vector Network Analyzer to validate the proposed theory. The measured data are further analyzed with respect to the limitations in fabrication such as tolerances in (sensitivity to) width and spacing of the conductor, and the height of the dielectric.

Chapter Six includes conclusion and suggestions for future work.

2. REVIEW OF CONVENTIONAL POWER DIVIDERS

2.1. Introduction

RF power dividers and combiners are passive RF devices that divide an RF signal into two or more RF signals of less power or combine several signals into a single signal of more power. The most common type of power divider is the equal split (3 dB) power divider rather than an unequal power divider. Although power dividers could be composed of 90 deg hybrids, the term "power divider" normally refers to a device that splits an input signal into two or more in-phase outputs. The term "isolation" defines the isolation between any set of output ports. It is the ratio, expressed in decibels, of the output power of one output port to any other output port, with matched terminations at all other ports. Isolation is important since a mismatched output port can affect the other output port signals.

A number of different types of power dividers have been realized over the years. In particular, realizations in planar transmission line technology are attractive because of the ease in fabrication and integration with other circuit components.

The Wilkinson power divider [8] is a popular type of power divider in planar technology used at microwave frequencies. It can ideally achieve perfect isolation between the output ports at the design frequency but is useful only over a limited bandwidth. To increase the useful bandwidth, two or more power divider sections can be cascaded. A further disadvantage of the Wilkinson power divider is that it requires a cross-over for the isolation resistor when it has three or more output ports (3-way Wilkinson divider) [14].

In this chapter, several conventional power dividers are reviewed, and the basic operation principle is described. In particular, the basic theory of the Wilkinson power divider is described in more detail as it is the basis of this thesis.

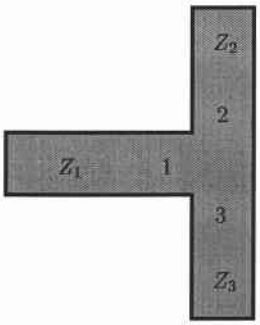

FIGURE 2.1. T-junction power divider

2.2. T-Junction Power Divider

The simplest type of power divider is the three-port lossless T-junction power divider as shown in Figure 2.1 [9]. If discontinuity effects at the junction are negligible, the input impedance at input port 1 is

$$Z_{in,1} = \frac{Z_2 Z_3}{Z_2 + Z_3}. \tag{2.1}$$

If input port 1 is matched ($Z_{in,1} = Z_1$), and the voltage at the junction is V_0, the input power at port 1 is

$$P_1 = \frac{1}{2}\frac{V_0^2}{Z_1}. \tag{2.2}$$

Thus, the output powers at ports 2 and 3 are respectively,

$$P_2 = \frac{Z_1}{Z_2} P_1, \tag{2.3}$$

$$P_3 = \frac{Z_1}{Z_3} P_1. \tag{2.4}$$

Various power divisions can be made by choosing the ratios of Z_1, Z_2, and Z_3. A 3 dB power split can be achieved, for example, when $Z_2 = Z_3 = 2Z_1$. The power will split evenly into the arms of the T with each arm having half the original power.

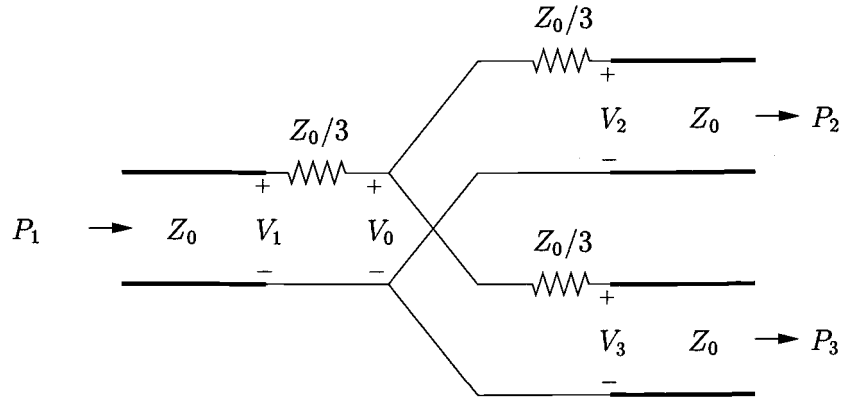

FIGURE 2.2. Resistive power divider

In this case, the input port is matched ($Z_{in,1} = Z_1$). However, the input impedances at the other two ports are not matched, and there is no isolation between the two output ports.

To have a matching condition for all ports, a resistive power divider network can be used, as shown in Figure 2.2. Assuming all ports are matched into characteristic impedance Z_0, each arm section without the resistors would see an unmatched termination of $1/2Z_0$. If a resistor $Z_0/3$ is connected in series to each line as shown, the input impedance $Z_{in,arm}$ of each arm seen from the junction to the output port is

$$Z_{in,arm} = \frac{Z_0}{3} + Z_0 = \frac{4Z_0}{3}. \tag{2.5}$$

Then, the input impedance of the power divider at the input port is

$$Z_{in} = \frac{Z_0}{3} + \frac{2Z_0}{3} = Z_0 \tag{2.6}$$

i.e., the input port is matched to Z_0. Due to the symmetry of the network, all ports are matched in the same way.

Assuming the voltage at the junction is V_0, it can be expressed as voltage division as

$$V_0 = \frac{2Z_0/3}{Z_0/3 + 2Z_0/3} V_1 = \frac{2}{3} V_1, \tag{2.7}$$

where V_1 is the voltage at the input port, and the term $2Z_0/3$ is from the parallel connection of two arms using Equation (2.5). In a similar way, the voltages at the output ports are found as

$$\begin{aligned} V_2 = V_3 &= \frac{Z_0}{Z_0 + Z_0/3} V_0 = \frac{3}{4} V_0 \\ &= \frac{1}{2} V_1. \end{aligned} \tag{2.8}$$

Thus, the input power at port 1 is

$$P_1 = \frac{1}{2} \frac{V_1^2}{Z_0} \tag{2.9}$$

and the output powers at ports 2 and 3 are

$$\begin{aligned} P_2 = P_3 &= \frac{1}{2} \frac{V_2^2}{Z_0} = \frac{1}{2} \frac{(1/2V_1)^2}{Z_0} = \frac{1}{8} \frac{V_1^2}{Z_0} \\ &= \frac{1}{4} P_1. \end{aligned} \tag{2.10}$$

Therefore, only a quarter of the input power, i.e. 6 dB, is delivered to each output port, and the other half of the input power is dissipated in the resistors. As a result, the T-junction power divider is quite easy to realize but either it can not have all ports matched or it is lossy with all ports matched. Also, it does not offer isolation between the two output ports.

2.3. Wilkinson Power Divider

A power divider often used at microwave frequencies is the Wilkinson power divider as mentioned in the previous chapter. Unlike the lossless T-junction divider,

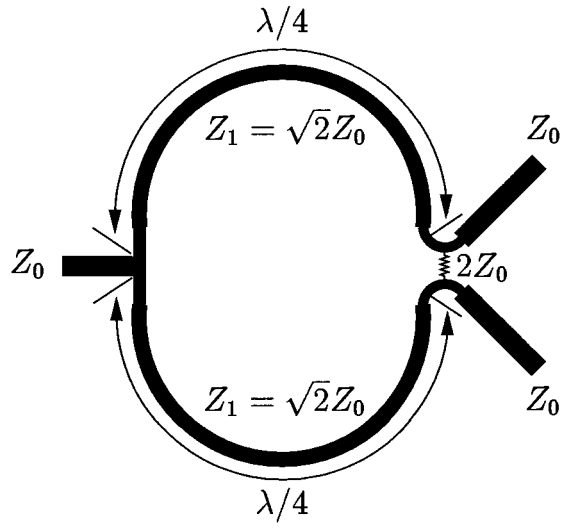

FIGURE 2.3. The 3 dB Wilkinson power divider

the Wilkinson power divider can have all ports matched and have perfect isolation between two output ports. The basic equal-split (3 dB) Wilkinson power divider is shown in Figure 2.3. The conventional design of the two-way Wilkinson power divider consists of two quarter-wave transmission-line sections and an isolation resistor between the two output ports. A brief analysis of the Wilkinson power divider is given below.

When the two output ports are matched, the two terminals of the resistor are at the same potential, which means that there is no current flow through the resistor. Thus, ignoring the resistor, the circuit has two parallel connected arms consisting of quarter-wavelength lines. If the characteristic impedance of each quarter-wavelength line is $\sqrt{2}Z_0$, the input impedance of each arm can be calculated as $Z_{in,arm} = 2Z_0$, since the input impedance of a quarter-wavelength transformer is

$$Z_{in} = \frac{Z_{T.L.}^2}{Z_{term}} = \frac{Z_1^2}{Z_0} \tag{2.11}$$

As a result, the total input impedance seen at the input port looking toward the output ports is matched to Z_0 because of the parallel connection of two arms. In other words, there is no reflection at the input port ($s_{11} = 0$).

The matching problem in the two output ports can be analyzed by even- and odd-mode analysis [15]. The even mode is defined when the two output ports are excited by the same voltage, and the odd mode is given by excitation with the same voltage magnitude but with opposite polarity. To analyze the network, we consider each mode separately, and then superimpose them later. For the even mode, the Wilkinson power divider can be bisected with an open circuit at the symmetry plane as shown in Figure 2.4 (a), since the voltage levels at the two ends of the resistor are equal. Also, the characteristic line impedance at the input port should be doubled to $2Z_0$ in this case, because it is expressed as a parallel connection of two identical impedances for the bisection. With the open-circuited end, half of the isolation resistor in the bisected circuit can be ignored, so that the input impedance at each output port is

$$Z_{in,2} = \frac{Z_{T.L.}^2}{Z_{term}} = \frac{Z_1^2}{2Z_0} \tag{2.12}$$

If the characteristic impedance of each quarter-wave section is $\sqrt{2}Z_0$, the input impedance becomes

$$Z_{in,2} = \frac{\left(\sqrt{2}Z_0\right)^2}{2Z_0} = Z_0 \tag{2.13}$$

Thus, each output port is matched to Z_0 for even-mode excitation.

Similarly, for odd-mode excitation, the structure can be bisected with ground connections in the symmetry plane as shown in Figure 2.4 (b), since there are voltage nulls. With the input port short-circuited, the quarter-wave transmission line can be ignored at the output port, since it acts like an opencircuit after the quarter-wavelength. All current will be delivered to the isolation resistor. If we choose the

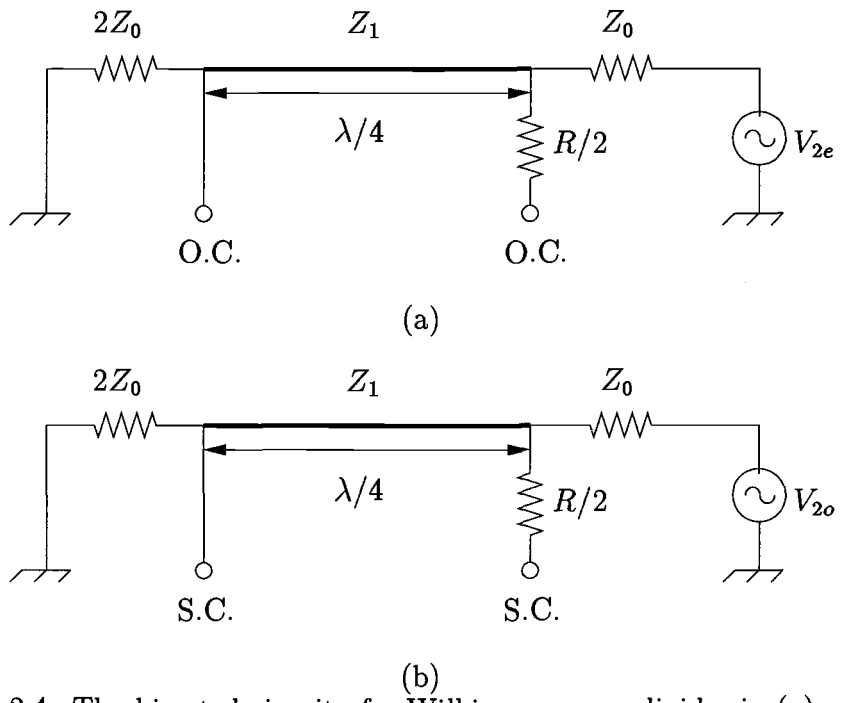

FIGURE 2.4. The bisected circuit of a Wilkinson power divider in (a) even mode excitation, (b) odd mode excitation.

resistor value $R/2$ as Z_0, the input impedance at the output port will be matched to Z_0 for odd mode excitation. The symmetry of the bisected circuit will give the same result for other output port. Thus, each output port is matched to Z_0 for odd mode excitation. As a result, the two output ports of the Wilkinson power divider are matched ($S_{22} = S_{33} = 0$).

For power division from the input port to the output port, the voltages at each port need to be found. The voltage of a traveling wave on a transmission line, when it is terminated with load Z_L, is given as

$$\begin{aligned} V_z &= V_o^+ e^{-j\beta z} + V_o^- e^{j\beta z} \\ &= V_o^+ \left[e^{-j\beta z} + \Gamma e^{j\beta z} \right] \end{aligned} \tag{2.14}$$

where Γ is the voltage reflection coefficient given as

$$\Gamma = \frac{V_o^-}{V_o^+} = \frac{Z_L - Z_0}{Z_L + Z_0} \tag{2.15}$$

Defining $z = 0$ at the input port and $z = -\lambda/4$ at the output port, Equation (2.14) for even-mode excitation gives

$$\begin{aligned} V_2^e &= V(-\lambda/4) = V_o^+ \left[e^{j\pi/2} + \Gamma e^{-j\pi/2} \right] \\ &= jV_o^+ (1 - \Gamma) \end{aligned} \tag{2.16}$$

With this, the voltage at the input port can be expressed as

$$\begin{aligned} V_1^e &= V(0) = V_o^+ (1 + \Gamma) \\ &= jV_2^e \frac{\Gamma + 1}{\Gamma - 1} \end{aligned} \tag{2.17}$$

From Equation (2.15), the voltage reflection coefficient Γ is given as

$$\Gamma = \frac{2Z_0 - Z_1}{2Z_0 + Z_1} = \frac{2 - \sqrt{2}}{2 + \sqrt{2}} \tag{2.18}$$

if $Z_1 = \sqrt{2}Z_0$. Finally, Equation (2.17) becomes

$$V_1^e = -jV_2^e\sqrt{2} \tag{2.19}$$

For odd-mode excitation, the voltage at the output port is the same as for even-mode excitation. Therefore, the quarter-wavelength line can be ignored. Also, the voltage at the input port is zero because of the short-circuit condition. Thus,

$$\begin{aligned} V_2^o &= V_2^e \\ V_1^o &= 0 \end{aligned} \tag{2.20}$$

If we superimpose even- and odd-mode excitation, the power delivered from one output port to the input port in terms of S-parameters is given as

$$S_{12} = S_{21} = \frac{V_1^e + V_1^o}{V_2^e + V_2^o} = -j/\sqrt{2} \tag{2.21}$$

Finally, when the output ports are matched, they are isolated by the open-circuit and the short-circuit conditions at the bisection for each mode respectively, ($S_{23} = 0$). When either port is not matched, the difference of the two output ports will go through the isolation resistor and the power will be dissipated there.

The complete S-parameters of the Wilkinson power divider at the design frequency for matched ports are given as

$$[S] = \begin{bmatrix} 0 & -j/\sqrt{2} & -j/\sqrt{2} \\ -j/\sqrt{2} & 0 & 0 \\ -j/\sqrt{2} & 0 & 0 \end{bmatrix} \tag{2.22}$$

This matrix satisfies the unitary condition for a lossless network. The design conditions for the 3 dB Wilkinson power divider are

$$Z_1 = \sqrt{2}Z_0$$
$$R = 2Z_0$$
$$l = \lambda/4 \tag{2.23}$$

2.4. Conclusion

Three conventional types of power dividers have been reviewed and their properties have been analyzed. The T-junction power divider can either be lossless but with not all ports matched, or with at all ports matched but lossy. The Wilkinson power divider has the advantage of isolation between two output ports over the T-junction power divider. In addition, when all ports are matched and only the input port is excited, the Wilkinson power divider is a lossless network. For ideal operation, the Wilkinson power divider needs to have two quarter-wavelength transmission lines with characteristic impedance $\sqrt{2}Z_0$, and an isolation resistor of $R = 2Z_0$. Because of the wavelength dependence, the quarter-wave sections occupy a large space at lower RF frequencies. To make the Wilkinson power divider more compact, the quarter-wave sections can be folded. The basic theory of a single folded-line section is given in the next Chapter. The folded-line power divider design is described in Chapter Four.

3. ANALYSIS OF GENERAL FOLDED-LINE STRUCTURES

3.1. Introduction

This chapter presents a general approach for the folded-line structure by network representation of the corresponding multiple coupled transmission lines. The size issue for conventional passive component circuit designs at RF stated in the previous chapter can be solved by adapting folded-lined structures. The concept of folded lines is introduced in terms of multiple coupled transmission lines that are interconnected at the ends with single transmission lines. A single C-section consisting of two coupled lines and with ideal interconnection at one end is introduced as the basic building block, and its two-port chain matrix (ABCD) is derived. To realize this basic C-section block in an actual circuit, an additional transmission line for the interconnection part between two ends of the coupled transmission line is introduced. Comparison has been made between the ideal and practical C-section to evaluate the performance of the folded-line structure and demonstrate the feasibility of the folded-line concept.

3.2. Network Representation of a General Folded-Line Structure

The general design methodology for embedded passive components consisting of folded lines is based on a network description of the corresponding multiple coupled transmission lines. For example, for the folded-line configurations shown in Figure 3.1, a folded line with $N-1$ folds consists of N coupled lines. The figure shows possible folded-line geometries with lines folded in edge and broad-side coupled configurations. Depending on the interconnections between each line in the

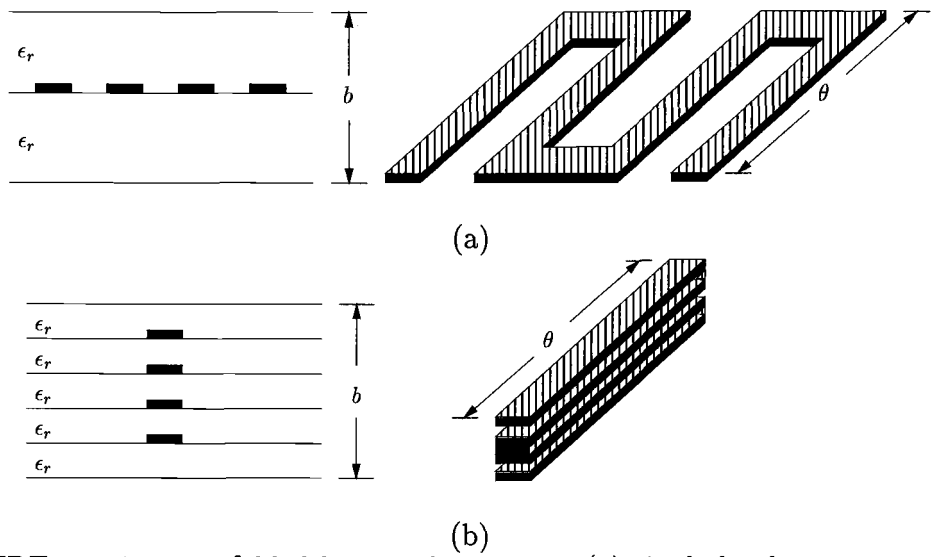

FIGURE 3.1. Various folded-line configurations: (a) single level structure and (b) multi-level structure.

folded structure, the entire network can have different properties, which can be used in the design of various embedded passive components.

A general approach for modeling a $2N$-port system associated with N multiple coupled lines using network parameters is well established [16, 17]. The circuit parameters of this $2N$-port network can be fully described either by the normal-mode parameters or via the inductance and the capacitance matrics of the N coupled line system. For the special case of N coupled lines in a homogeneous medium, such as in a stripline environment, the capacitance matrix and the phase velocity completely describe the corresponding $2N$-port network. The $2N \times 2N$ admittance parameter matrix can be expressed as

$$[Y]_{2N\times 2N} = \frac{1}{\sqrt{\epsilon_r \epsilon_o \mu_o}} \begin{bmatrix} [C]_{N\times N}\coth(\gamma l) & -[C]_{N\times N}\operatorname{csch}(\gamma l) \\ -[C]_{N\times N}\operatorname{csch}(\gamma l) & [C]_{N\times N}\coth(\gamma l) \end{bmatrix} \tag{3.1}$$

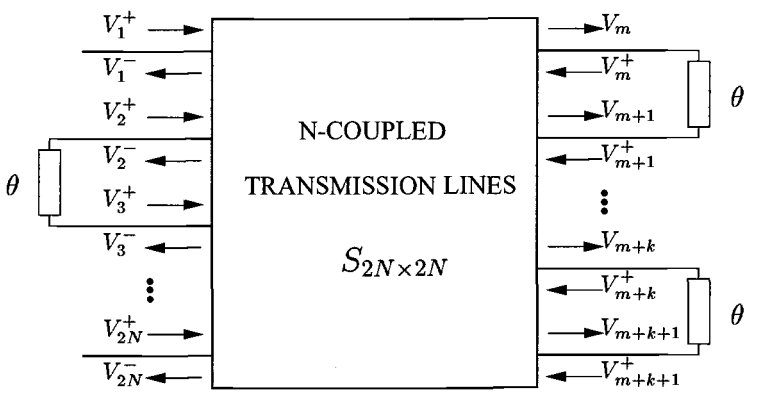

FIGURE 3.2. Network representation for a general folded-line configuration.

where $[C]_{N\times N}$ is the capacitance matrix of the N coupled line structure, l is the length, and γ is the propagation constant. The scattering matrix $[S]_{2N\times 2N}$ can be directly derived from the expression for the admittance matrix shown in Equation (3.1). Similar expressions in terms of the capacitance and inductance matrices can be derived for inhomogeneous media. The capacitance matrix in Equation (3.1) can be derived by several quasi-static or approximate closed-form formulations [18, 19] for a multi-conductor transmission line system in homogeneous and inhomogeneous media.

Figure 3.2 shows the network representation of a folded line with $N-1$ folds, in terms of the $[S]_{2N\times 2N}$ scattering matrix of the corresponding N coupled line structure. Depending on the location of the folds, the corresponding ports are connected via an equivalent length of transmission line with electrical delay identical to that of the bend. The reduced 2×2 scattering matrix of the folded-line section can be obtained by selectively eliminating the unknown incident and reflected wave amplitudes at the connected ports and relating the incident and

reflected amplitudes at the input and output ports. For simplification of the whole procedure, a transmission line with one fold is considered as a single C-section with two coupled lines of equal width, which are connected at one of the ends. A transmission line with many folds can be considered as cascades of C-sections provided the coupling between the C-sections is negligible.

3.3. Analysis of a Single C-Section Block with Ideal Connection

If only one fold is considered, the C-section can be idealized simply as two coupled transmission lines with ideal interconnection at one end by assuming negligibly small connecting-through section length compared to the wavelength, as shown in Figure 3.3 (c). With this assumption, a simple form of the 2×2 chain matrix is obtained for an ideal C-section. This form is beneficial for getting simple closed-form design equations.

The symmetric coupled transmission lines are often described by even- and odd-mode impedances for the stripline configuration, since the even- and odd-mode impedances can be directly transformed into physical design parameters of the coupled stripline for given dielectric constant and frequency. Once the chain matrix of the coupled transmission line is expressed in terms of even- and odd-mode impedances, the design equations for the entire passive component are also given in terms of even- and odd-mode impedances. Thus, the realization of the passive component is achieved by a simple transformation from electrical parameters to physical parameters.

To obtain the chain matrix of an idealized C-section, an analysis of the four-port coupled line system is needed. A parallel coupled-line section with port voltage and current definition is shown in Figure 3.3 (a). Using the method of even- and odd-

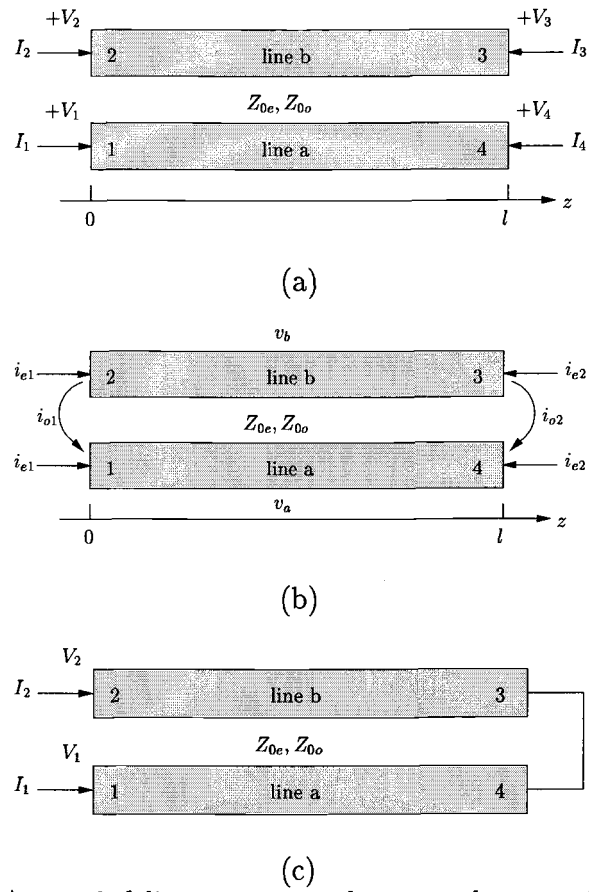

FIGURE 3.3. (a) A coupled-line section with port voltage and current definition. (b) A coupled-line section with even- and odd-mode current sources. (c) A two-port coupled-line section with a ideal connection at one end.

mode excitations of the coupled-line system, the four-port open-circuit impedance matrix can be obtained as follows [9].

If even-mode excitation with the i_{e1} current sources is considered, the input impedance seen at port 1 or 2, when all other ports are open-circuited, is

$$Z_{in}^{e} = -jZ_{0e}\cot(\beta l). \tag{3.2}$$

The voltage on either conductor (line a or line b) at port 1 or 2 can be expressed as

$$v_a^{e1}(0) = v_b^{e1}(0) = Z_{in}^e \times i_{e1}$$
$$= -jZ_{0e}\cot(\beta l) \times i_{e1}, \tag{3.3}$$

By evaluating the ABCD parameters of the two-port network, the voltages at ports 3 or 4 for this even-mode excitation current i_{e1} can be obtained as

$$v_a^{e1}(l) = v_b^{e1}(l) = -jZ_{0e}\csc(\beta l) \times i_{e1}. \tag{3.4}$$

Similarly, the voltages at port 1 or 2 due to the current source i_{e2} driving the line in the even mode are

$$v_a^{e2}(0) = v_b^{e2}(0) = -jZ_{0e}\csc(\beta l) \times i_{e2}, \tag{3.5}$$

and the voltages at port 3 or 4 are

$$v_a^{e2}(l) = v_b^{e2}(l) = -jZ_{0e}\cot(\beta l) \times i_{e2}. \tag{3.6}$$

When odd-mode excitation by i_{o1} current source is considered, the impedance seen at port 1 or 2 with the other ports open-circuited is

$$Z_{in}^o = -jZ_{0o}\cot(\beta l). \tag{3.7}$$

Thus, the voltages due to i_{o1} at ports 1 and 2 can be expressed as

$$v_a^{o1}(0) = -v_b^{o1}(0) = -jZ_{0o}\cot\beta l \times i_{o1}, \tag{3.8}$$

and the voltages at ports 3 and 4 are

$$v_a^{o1}(l) = -v_b^{o1}(l) = -jZ_{0o}\csc\beta l \times i_{o1}. \tag{3.9}$$

Also, the voltages at ports 3 and 4 can be calculated as

$$v_a^{o2}(0) = -v_b^{o2}(0) = -jZ_{0o}\csc\beta l \times i_{o2}, \tag{3.10}$$

$$v_a^{o2}(l) = -v_b^{o2}(l) = -jZ_{0o}\cot\beta l \times i_{o2} \tag{3.11}$$

To obtain the four-port open-circuit impedance matrix $[Z]_{4\times4}$ of the coupled line, the four-port network is expressed in terms of total port voltages and total port currents as

$$\begin{bmatrix} V_1 \\ V_2 \\ V_3 \\ V_4 \end{bmatrix} = \begin{bmatrix} Z_{11} & Z_{12} & Z_{13} & Z_{14} \\ Z_{21} & Z_{22} & Z_{23} & Z_{24} \\ Z_{31} & Z_{32} & Z_{33} & Z_{34} \\ Z_{41} & Z_{42} & Z_{43} & Z_{44} \end{bmatrix} \times \begin{bmatrix} I_1 \\ I_2 \\ I_3 \\ I_4 \end{bmatrix} \tag{3.12}$$

where the total port voltages are given as the sum of each voltage derived for even- and odd-mode excitation. With Equations (3.3) to (3.9), the total port voltages are found as

$$\begin{aligned} V_1 &= v_a^{e1}(0) + v_a^{e2}(0) + v_a^{o1}(0) + v_a^{o2}(0) \\ V_2 &= v_b^{e1}(0) + v_b^{e2}(0) + v_b^{o1}(0) + v_b^{o2}(0) \\ V_3 &= v_b^{e1}(l) + v_b^{e2}(l) + v_b^{o1}(l) + v_b^{o2}(l) \\ V_4 &= v_a^{e1}(l) + v_a^{e2}(l) + v_a^{o1}(l) + v_a^{o2}(l) \end{aligned} \tag{3.13}$$

The port currents in terms of even- and odd-mode currents are

$$\begin{aligned} I_1 &= i_{e1} + i_{o1} \\ I_2 &= i_{e1} - i_{o1} \\ I_3 &= i_{e2} - i_{o2} \\ I_4 &= i_{e2} + i_{o2} \end{aligned} \tag{3.14}$$

The result from Equation (3.12) by using Equation (3.13) and (3.14) gives the complete $[Z]_{4\times4}$ matrix as

$$Z_{11} = Z_{22} = Z_{33} = Z_{44} = -j/2(Z_{0e} + Z_{0o}) \cot\theta, \tag{3.15}$$

$$Z_{12} = Z_{21} = Z_{34} = Z_{43} = -j/2(Z_{0e} - Z_{0o}) \cot\theta, \tag{3.16}$$

$$Z_{13} = Z_{31} = Z_{24} = Z_{42} = -j/2(Z_{0e} - Z_{0o}) \csc\theta, \tag{3.17}$$

$$Z_{14} = Z_{41} = Z_{23} = Z_{32} = -j/2(Z_{0e} + Z_{0o}) \csc\theta, \tag{3.18}$$

where $\theta = \beta l$.

If port 2 and port 3 are ideally connected to each other as shown in Figure 3.3 (c), the four-port $[Z]$ matrix can be reduced into a two-port $[Z]$ matrix, using the following relationships :

$$V_3 = V_4 \tag{3.19}$$

and

$$I_3 = -I_4. \tag{3.20}$$

The corresponding reduced $[Z]_{2\times2}$ matrix is

$$Z_{11} = Z_{22} = \frac{-j}{2}\left(\frac{Z_{0e} - Z_{0o}tan^2\theta}{\tan\theta}\right), \tag{3.21}$$

$$Z_{12} = Z_{21} = \frac{-j}{2}\left(\frac{Z_{0e} + Z_{0o}tan^2\theta}{\tan\theta}\right). \tag{3.22}$$

As a result, the two-port chain matrix (ABCD) transformed from Equation (3.21), and (3.22) is

$$[M] = \frac{1}{Z_{0e} + Z_{0o}\tan^2\theta}\begin{bmatrix} Z_{0e} - Z_{0o}\tan^2\theta & 2jZ_{0e}Z_{0o}\tan\theta \\ 2j\tan\theta & Z_{0e} - Z_{0o}\tan^2\theta \end{bmatrix} \tag{3.23}$$

In the following Chapter, this 2×2 chain matrix will be used to represent a single C-section for simplicity of calculation, even though it does not exactly represent the actual C-section.

The response comparison between a quarter-wavelength transmission line and an ideal C-section (a coupled line with ideal connection at one end) is shown in Figure 3.5. The two responses match well, especially at the aimed center frequency. This demonstrates the behavior of the C-section as a substitute for a quarter-wavelength transmission-line section. It is clearly seen that it would be impossible to implement an ideal C-section. For the implementation of a C-section in a real design, a transmission-line connection at one end of the coupled lines needs to be introduced. The effect and the compensation for this transmission-line connection will be discussed in the next section.

3.4. Analysis of a C-section Block with Transmission Line Connection

In the actual realization of the C-section, the length of the through connection may be a significant fraction of the length of the coupled line section and, thus, may not be neglected. An adjustment of the length of the coupled line would not be sufficient to get the response of an ideally connected C-section. To realize the C-section, the C-section with transmission line connection is segmented as shown in Figure 3.4. For the interconnecting part, the connection between the coupled line is composed of two 90 degree bends and a through transmission line. For easier connection with other components, two more 90 degree bends have been added at the other end of the coupled line, as shown in Figure 3.4 (b). The response of the ideal C-section and realized C-section before tuning for W and S is compared with that of a $\lambda/4$ line in Figure 3.5.

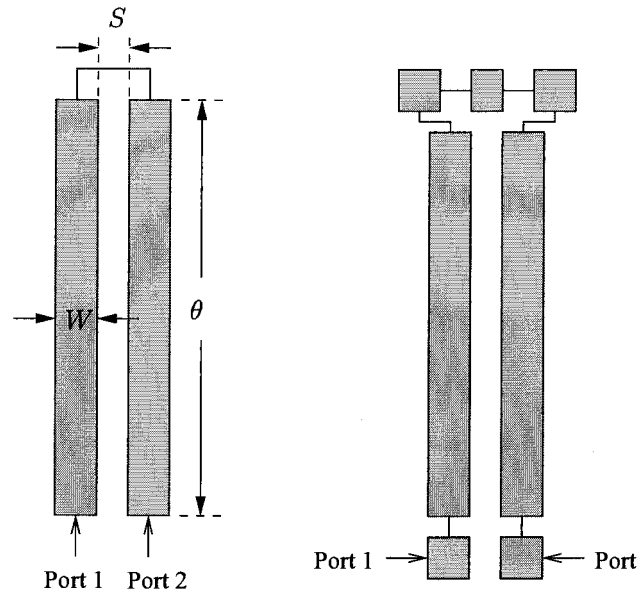

(a) (b)

FIGURE 3.4. Configuration of (a) idealized C-section, and (b) segmentation of a C-section with non-negligible through-connection length.

Since the connecting-through transmission line causes impedance mismatch between the coupled lines, compensation is achieved by tuning of W and S of the coupled line. In addition, the additional coupling length caused by the 90 degree bends needs to be compensated by decreasing the length of the coupled line accordingly. After tuning of W, S, and θ of the coupled line, the response of the C-section with transmission-line connection is matched to that of the ideal C-section, as shown in Figure 3.6. More details on tuning of W, S, and θ of the coupled line will be discussed in Chapter Four.

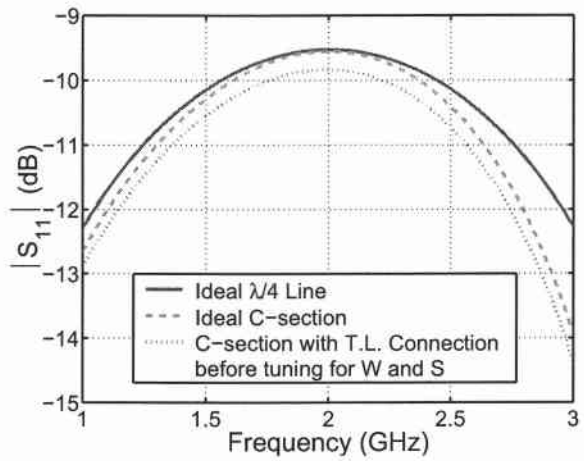

(a)

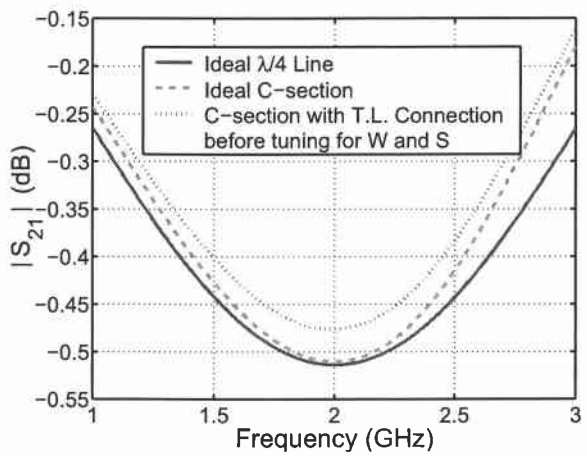

(b)

FIGURE 3.5. Response of a single C-section before tuning of w and s of the coupled line: (a) S_{11}, (b) S_{22}.

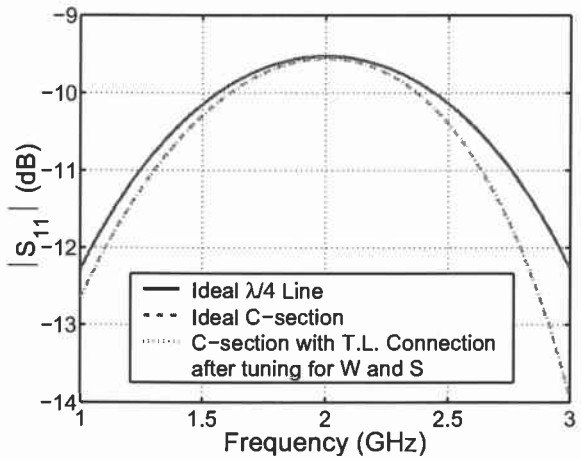

(a)

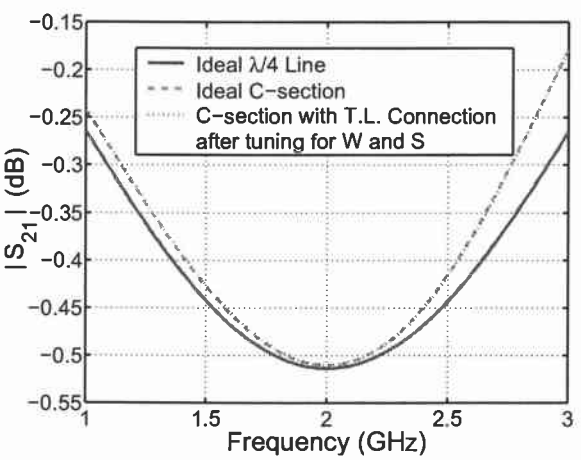

(b)

FIGURE 3.6. Response of a single C-section after tuning of w and s of the coupled line: (a) S_{11}, (b) S_{22}.

3.5. Conclusion

A general approach for a folded-line structure by network representation of the corresponding multiple coupled transmission lines has been presented. The concept of folded lines as cascaded C-sections is introduced. For each C-section the coupled transmission lines are connected at one end with a transmission line section. One C-section with ideal connection has been analyzed first to use as a basic building block, and its two-port chain (ABCD) matrix has been derived. An additional transmission line for the interconnection between the two ends of the coupled transmission lines is introduced to realize the basic C-section block in a physical environment. Comparison has been made between the ideal and practical C-section to demonstrate the feasibility of the folded-line concept. The coupled-line dimensions have been tuned to compensate for the non-ideal connections.

4. DESIGN OF SINGLE LEVEL AND TWO-LEVEL 3DB POWER DIVIDERS USING FOLDED-LINES

4.1. Introduction

In this chapter, the design procedure for the conventional Wilkinson 3dB power divider is briefly reviewed. Based upon the properties of the C-section described in Chapter Three, the design procedure for the new compact RF power divider using folded lines in single- and multi-level configuration is studied. New simple closed-form design equations for the 3dB power divider for both one C-section and two cascaded C-sections are developed. Based on these design equations, design examples for the 3dB power divider are presented for each case. Furthermore, other design issues including physical layout geometries and tuning for optimal response are discussed. The full-wave electromagnetic simulator *Momentum* is used for preliminary validation. The size reduction in footprint of the layout is also presented.

4.2. Design of Conventional Wilkinson 3dB Power Divider

The Wilkinson power divider is a solution to the lossless T-junction divider, which is not matched and has non-isolated output ports. The resistive T-junction divider solves the matching problem, but does not offer isolation. Furthermore, this solution leads to power loss because of the resistive structure of the resistive T-junction divider. The Wilkinson power divider is a three port network, which has the property of being lossless when the source is connected to the input port and the output ports are matched. In addition, isolation between the output ports can be achieved by a resistor, which will dissipate any reflected power from the output ports. There are two general types of the Wilkinson power divider; the equal power

divider and the unequal power divider. In this thesis, the equal split (3 dB) Wilkison power divider is discussed.

As discussed in Chapter Two, the conventional Wilkinson power divider is composed of two quarter-wavelength transmission lines and one isolation resistor. To achieve the 3 dB power divider characteristics given in Equation (2.22) at the design frequency, the quarter-wavelength transmission line should have the characteristic impedance

$$Z_1 = \sqrt{2}Z_0 = 70.7\Omega \tag{4.1}$$

and the isolation resistor value should be

$$R = 2Z_0 = 100\Omega \tag{4.2}$$

where $Z_0 = 50\Omega$ is the system impedance. Note that since the quarter-wavelength transmission lines are frequency dependent, the S-parameters are also frequency dependent.

In the design of this Wilkinson power divider, the stripline configuration has been chosen for future extension to the multi-level layer cases. Once the characteristic impedances of the quarter-wavelength line and the isolation resistor value are obtained, the physical dimensions of the transmission lines for the given stripline environment and operating frequency are found. There are several methods to formulate the relationship between the characteristic impedance and the physical geometry of the stripline. One possibility is to use a conformal mapping approach [20], which can give an exact solution of Laplace's equation for TEM waves. The other approach is to use various numerical methods. However, both of these procedures are beyond the scope of this thesis. Here, the commercial software *LineCalc* [21] has been used. This software is an analysis and synthesis program for calculating the

TABLE 4.1. Physical geometry of a conventional Wilkinson power divider in stripline configuration ($\epsilon_r = 2.2, f_c = 2$ GHz).

Width or Length	Value (mil)
W_0 ($Z_0 = 50\Omega$)	51.41
W_1 ($Z_1 = \sqrt{2}Z_0 = 70.7\Omega$)	28.55
L ($\lambda/4$)	994.69
b (ground spacing)	62

electrical and physical parameters of several types of single and coupled transmission lines. It can produce required physical geometries for a stripline configuration. Here, a homogeneous dielectric medium $\epsilon_r = 2.2$ with ground separation $b = 62mil$ is considered for the stripline configuration, and the design frequency is chosen as 2 GHz.

The conventional Wilkinson power divider design is summarized in Table 4.1, and its layout is shown in Figure 4.6 (a). The ideal response of the Wilkinson power divider simulated in ADS [21] is shown in Figure 4.1. As expected, the reflection at port 1 and the isolation between port 2 and 3 are negligible at the operation frequency of 2 GHz. Also, the power divisions at ports 2 and 3 are half of original power (3 dB) at the design frequency.

4.3. Design of Single Level 3dB Power Divider with Single C-section

This section presents the procedure for designing a 3 dB Wilkinson power divider using a single C-section discussed in Chapter Three. The following new compact RF power dividers in single level have also been published in [22]. The

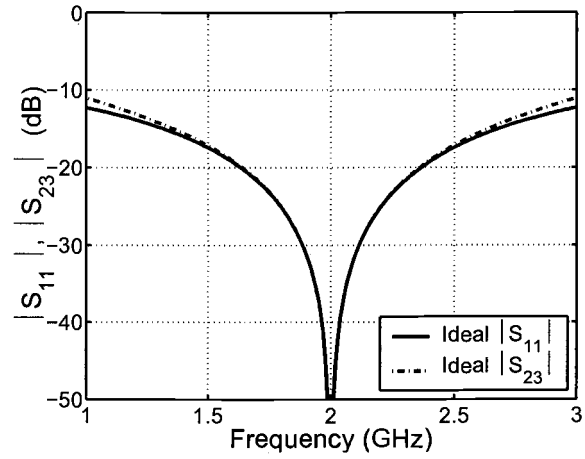

(a)

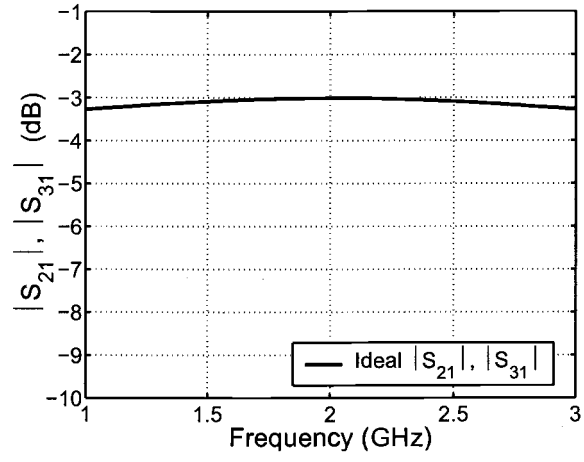

(b)

FIGURE 4.1. Ideal response of a 3 dB Wilkison power divider: (a) $|S_{11}|, |S_{23}|$, (b) $|S_{21}|, |S_{31}|$.

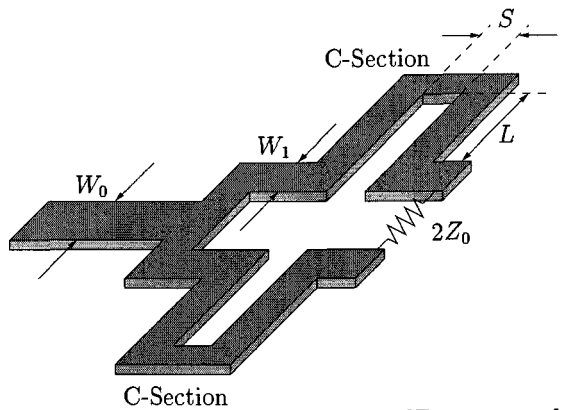

FIGURE 4.2. Configuration of the compact 3 dB power divider with a single C-section.

simple configuration of the proposed compact 3 dB power divider with a single C-section is shown in Figure 4.2. The main idea is to replace the quarter-wavelength line with a C-section, while the other parts of the power divider remain the same. This gives a more compact size for the conventional quarter-wavelength lines and hence, the power divider.

The two-port quarter-wavelength line can be represented by 2×2 ABCD parameters as [9]

$$\begin{bmatrix} A & B \\ C & D \end{bmatrix} = \begin{bmatrix} \cos\beta l & jZ_0 \sin\beta l \\ jY_0 \sin\beta l & \cos\beta l \end{bmatrix} \tag{4.3}$$

where $\beta = \omega/v_p = 2\pi/\lambda$, and $l = \lambda/4$ at the center frequency. The electrical length θ at the center frequency is

$$\theta = \beta l = \pi/2 = 90^\circ \tag{4.4}$$

As a result, from Equation (4.3), the ABCD matrix for a quarter-wavelength line at the center frequency becomes

$$[M_1] = \begin{bmatrix} 0 & j\sqrt{2} \\ \frac{j}{\sqrt{2}} & 0 \end{bmatrix} \tag{4.5}$$

In Chapter Three, the two-port chain (ABCD) matrix of an ideal C-section has been derived, see Equation(3.23). Comparing Equations (3.23) and (4.5), the even- and odd-mode characteristic impedances of the C-section are obtained as

$$Z_{0e} = \sqrt{2} Z_0 \tan\theta \tag{4.6}$$

$$Z_{0o} = \frac{\sqrt{2} Z_0}{\tan\theta} \tag{4.7}$$

These two equations form the basic design equations of the 3 dB Wilkinson power divider with a single C-section. When θ is limited to $\pi/4$, Equations (4.6) and (4.7) reduce to those of the conventional un-coupled (unfolded) strip transmission line. It is interesting to consider the limitations in choosing the electrical length θ. When θ is smaller than $\pi/4$, the coupled line cannot be realized as seen in Equation (4.6) and (4.7), since this would result in $Z_{0e} < Z_{0o}$. Therefore, θ should be greater than $\pi/4$ for the design.

As an example, a 3dB power divider using a single C-section has been designed using Equations (4.6) and (4.7). The design parameters have been chosen as $\theta = 50°$ for the electrical length of each C-section and $f_c = 2$ GHz for the center frequency. The physical dimensions of this design are summarized in Table 4.2.

As discussed in Chapter Three, the ideal C-section can replace the $\lambda/4$ length line by simply adjusting the physical parameters. Due to the assumption of an ideal C-section in the derivation of Equations (4.6) and (4.7), the physical dimensions of the C-sections in this design need to be further tuned. The tuning is done in the commercial simulator *ADS* using an equivalent circuit model for the C-section and

TABLE 4.2. Physical geometry of a 3 dB power divider using a single C-section ($\epsilon_r = 2.2, \theta = 50°$, and $f_c = 2$ GHz).

Width or Length	Value (mil)
W_0 ($Z_0 = 50\Omega$)	51.41
$W_1(Z_{oe} = 84.27\Omega, Z_{oo} = 59.33\Omega)$	27.12
S ($Z_{oe} = 84.27\Omega, Z_{oo} = 59.33\Omega$)	14.80
$L(50°)$	552.60
b (ground spacing)	62

TABLE 4.3. Physical geometry of a 3 dB power divider using a single C-section after tuning ($\epsilon_r = 2.2, f_c = 2$ GHz).

Width or Length	Value (mil)
W_0	51.41
W_1	26.23
S	13.58
L	443.0
b	62

connecting line segments. After the tuning process, a new set of physical parameters for the 3 dB power divider is obtained, as summarized in Table 4.3. The tuning procedure has been performed for the entire power divider circuit to observe the final response of the designed power divider.

The response comparison of this 3 dB power divider before and after tuning is shown in Figure 4.3. After tuning, the response of the compact power divider

with a single C-section agrees very well with that of the conventional design. It is intuitive that the response before tuning is shifted to lower frequencies, since the interconnection length and bends add an additional phase shift. Further details on the sensitivity of each physical parameter will be given in Chapter Five.

The layout of this new compact power divider with a single C-section is shown at Figure 4.6 (b). Compared to the area of a rectangle enclosing the conventional layout, a footprint reduction of about 67% is achieved with the compact design using single folded lines. However, the folded-line power divider extends farther in the vertical direction compared to the conventional design. A further reduction in footprint size can be achieved by using more folded lines instead of a single C-section. This will be discussed in the next section.

4.4. Design of Single Level 3dB Power Divider with Multi C-Sections

In this section, we will extend the concept of folded line (single C-section) to multiple folded lines to achieve more compact designs. Instead of a single C-section, two cascaded C-sections can be used to replace each quarter-wavelength line section in the previous power divider design. For simplicity, the three folded lines in a single layer as shown in Figure 4.4, can be treated as the cascade connection of two C-sections in series. If the cascaded C-sections are separated far enough, coupling effects between the two C-sections can be ignored. Otherwise, the folded-line system needs to be treated as a four-coupled-line system.

The procedure for getting design equations for the power divider with two cascaded C-sections is similar to the single C-section case. The 2×2 ABCD parameters of the cascaded C-sections can be expressed as

$$[M_{2c}] = [M_2]\,[M_2] \tag{4.8}$$

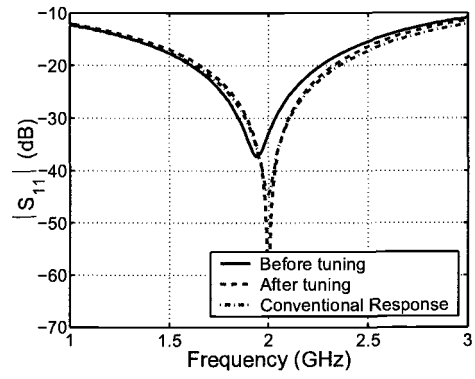

(a)

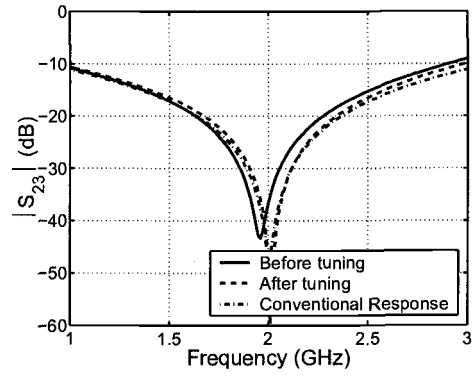

(b)

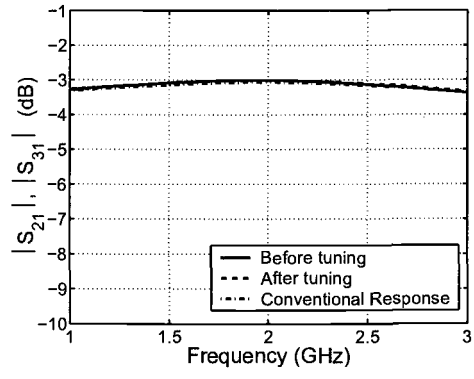

(c)

FIGURE 4.3. Response of the 3 dB power divider using a single C-section.

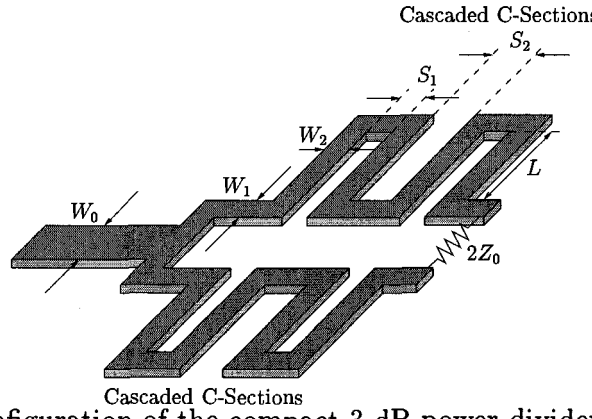

FIGURE 4.4. Configuration of the compact 3 dB power divider with two cascaded C-sections

where $[M_2]$ represents the ABCD parameters of a single C-section as given by Equation (4.5). From comparison of Equations (4.5) and (4.8), the ABCD parameters of an ideal single C-section, when two are cascaded, are obtained at the center frequency as

$$[M_2] = \begin{bmatrix} \frac{1}{\sqrt{2}} & j \\ \frac{j}{2} & \frac{1}{\sqrt{2}} \end{bmatrix} \tag{4.9}$$

By comparing the 2×2 ABCD parameters of an ideal C-section, Equations (3.23) and (4.9), simple closed-form design equations in terms of even- and odd-mode characteristic impedances are obtained as

$$Z_{0e} = \frac{\sqrt{2} Z_0 \tan\theta}{\sqrt{2} - 1} \tag{4.10}$$

$$Z_{0o} = \frac{\sqrt{2} Z_0 (\sqrt{2} - 1)}{\tan\theta} \tag{4.11}$$

where θ is the electrical length of each single C-section. These two equations will be used to obtain the physical dimensions of the power divider with two cascaded C-sections. Similar to the single C-section case, when θ is $\pi/8$, Equations (4.10) and (4.11) reduce to those of the conventional non-coupled strip transmission line. Thus, the choice of θ value is limited to be greater than $\pi/8$, or the edge coupled line in each C-section can not be realized, as seen from Equations (4.10) and (4.11).

As a design example, a 3 dB power divider with two cascaded C-sections has been designed. The electrical length of each C-section has been chosen as $\theta = 25$ deg for a center frequency of 2 GHz. From Equations (4.10) and (4.11), the physical parameters of the power divider with two cascaded C-sections are calculated and given in Table 4.4. The spacing between the cascaded C-sections is set to 60 mil to avoid coupling effects between the C-sections. After a simple tuning procedure, as explained for the case of a single C-section, the final design is obtained as shown in Table 4.5. It should be kept in mind that the spacing between two cascaded C-sections needs to remain the same during the tuning procedure to prevent coupling between the two C-sections.

The response computed by circuit simulation after tuning is shown in Figure 4.5. The response was also compared with the simulation results using the planar full-wave electromagnetic simulator *Momentum*. The responses are very close to each other. This comparison is sufficient as preliminary validation of the new design before fabrication.

The layout of the power divider with two cascaded C-sections is shown in Figure 4.6(c). Compared to the area of a rectangle enclosing the conventional layout, a footprint reduction of about 64% is achieved with the compact design using two cascaded folded lines. Even though the footprint area is slightly larger than that of the single C-section design, the dimensions of the power divider using cascaded

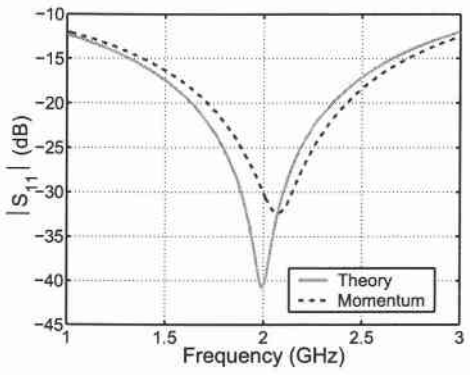

(a)

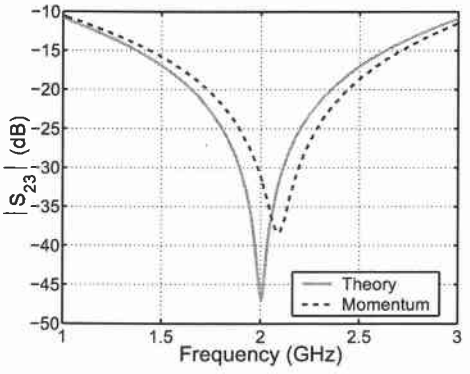

(b)

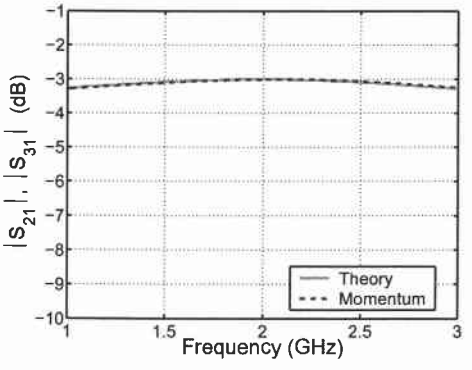

(c)

FIGURE 4.5. Response of the 3 dB power divider with two cascaded C-sections

TABLE 4.4. Physical geometry of a 3 dB power divider using two cascaded C-sections ($\epsilon_r = 2.2, \theta = 25°$, and $f_c = 2$ GHz)

Width or Length	Value (mil)
W_0 ($Z_0 = 50\Omega$)	51.41
$W_1 = W_2$ ($Z_{oe} = 79.60\Omega, Z_{oo} = 62.81\Omega$)	27.24
S_1 ($Z_{oe} = 79.60\Omega, Z_{oo} = 62.81\Omega$)	22.54
S_2 (spacing between C-sections)	60.0
$L(25°)$	276.3
b (ground spacing)	62

C-sections are nearly equally distributed. This should make it easier for component placement and more attractive to designers.

4.5. Design of a Two-Level 3dB Power Divider

In this section, we extend the idea of a single folded line to multiple folded lines in multiple conductor levels for more compact designs by taking advantage of the 3-D environment of the strip line configuration. The procedure of applying the folded-line concept to multiple conductor levels is also published in [23]. For the same even- and odd-mode characteristic impedances (Z_{0e}, Z_{0o}), the broadside-coupled line can have a more compact size in footprint compared to the edge-coupled line. The two different kinds of coupled-line configurations give an additional degree of design freedom. The simple configuration of the proposed compact two-conductor level 3 dB power divider with two cascaded C-sections is shown in Figure 4.7. After a single C-section is folded in the vertical direction (two different conductor levels),

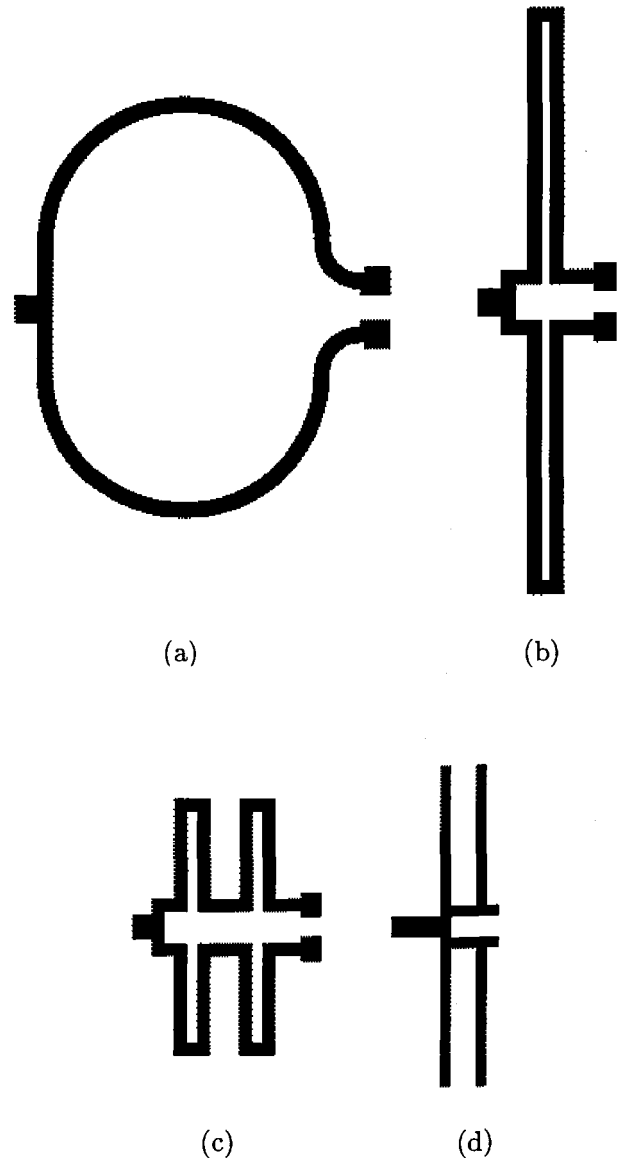

FIGURE 4.6. Comparison of footprint size of different power divider designs: (a) conventional design, (b) compact design with single C-section, (c) compact design with two cascaded C-sections, (d) compact design with two cascaded C-sections in two conductor level.

TABLE 4.5. Physical geometry of a 3 dB power divider using two cascaded C-sections after tuning ($\epsilon_r = 2.2, f_c = 2$ GHz)

Width or Length	Value (mil)
W_0	51.41
$W_1 = W_2$	26.41
S_1	20.27
S_2	60.0
L	180
b	62

two C-sections are cascaded in the horizontal direction. The design equations for the single conductor level cases can be used again, because the only difference is the physical realization from the edge-coupled-line configuration to the broadside-coupled-line configuration having the same electrical properties.

As a design example, a 3 dB power divider with two cascaded C-sections in two conductor levels has been considered. The electrical length of each C-section has been chosen as $\theta = 30°$ for a center frequency of 2 GHz. Also, the ground spacing b is chosen to be 60 *mil* with the height of each dielectric layer as 20 *mil*. From Equations (4.10) and (4.11), the same even- and odd-mode characteristic impedances as in the single level case are given. However, getting the physical dimensions from the even- and odd-mode characteristic impedances is more complicated than in the single level case, because of the lack of available models.

It is important to determine the conductor width for a $Z_0 = 50\Omega$ line in suspended substrate, as shown in Figure 4.8. Unfortunately, *LineCalc* does not offer

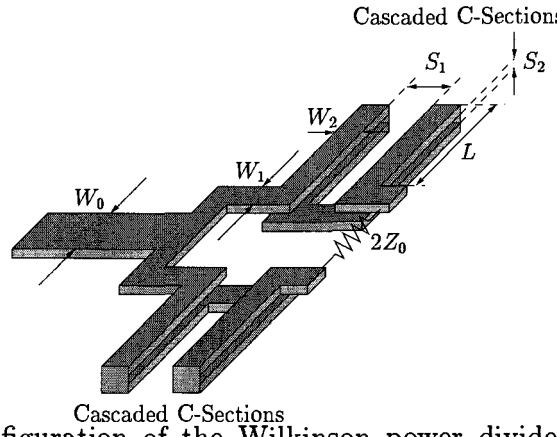

FIGURE 4.7. Configuration of the Wilkinson power divider with two cascaded C-sections in two conductor levels

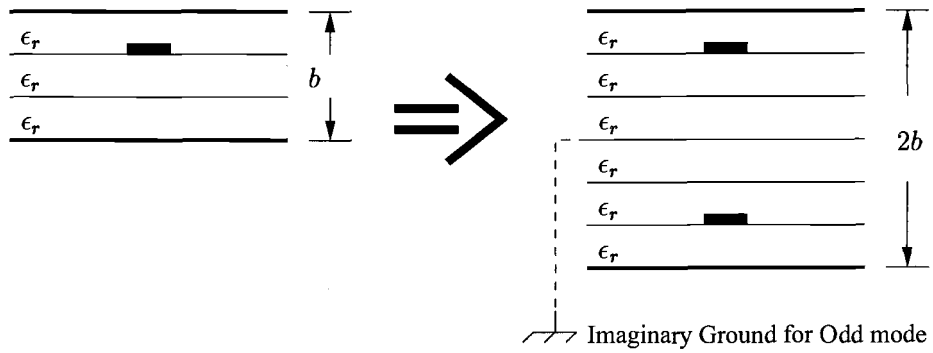

FIGURE 4.8. The conductor width of $Z_0 = 50\Omega$ line in suspended substrate

a model for this case, thus a broadside coupled line with twice of the ground spacing is considered. When odd-mode excitation is considered, the broadside coupled line will have a voltage null in the middle of the substrate, and it can be considered as the ground conductor in the suspended substrate case. Thus, the conductor width for $Z_0 = 50\Omega$ line can be taken from the conductor width of the broadside coupled line for $Z_{0o} = 50\Omega$ with doubled ground spacing.

The second thing to notice is that the two-conductor-level-case has one degree less design freedom, the spacing S between the coupled lines, than the single level

TABLE 4.6. Physical geometry of a two conductor level 3 dB power divider using two cascaded C-sections ($\epsilon_r = 2.2, \theta = 30°$, and $f_c = 2$ GHz)

Width or Length	Value (mil)
W_0 ($Z_0 = 50\Omega$)	42.9
W_1 ($Z_1 = \sqrt{2}Z_0 = 70.71\Omega$)	23.2
W_2 ($\sqrt{Z_{0e}Z_{0o}} = Z_1$)	21.12
S_1 (spacing between C-sections)	50.0
S_2 (fixed)	20.0
$L(30°)$	331.56
b (ground spacing)	60

case. Unlike the single level cases, the spacing S between the broadside-coupled line should be considered as design specification, since the height of each substrate layer is typically predetermined. With a fixed S, we can not have exactly the same even- and odd-mode characteristic impedances as those obtained from Equations (4.10) and (4.11). Therefore, the conductor width W of the broadside-coupled line is chosen so that the even- and odd-mode characteristic impedances for the given W satisfy the condition $\sqrt{Z_{0e}Z_{0o}} = Z_1$. As a final step, the length of the coupled lines is appropriately adjusted (tuned) to obtain effectively a quarter-wavelength at the design frequency. The resulting physical dimensions are summarized in Tables 4.6 and 4.7 for both before and after tuning.

The responses computed by both circuit simulation and the full-wave EM simulator *Momentum* after tuning are compared in Figure 4.9. The responses are found to be in very good agreement with each other. The layout of the two-

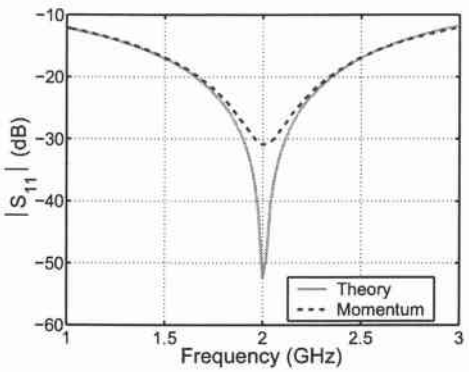

(a)

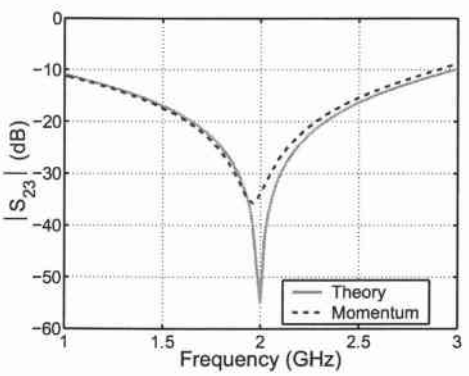

(b)

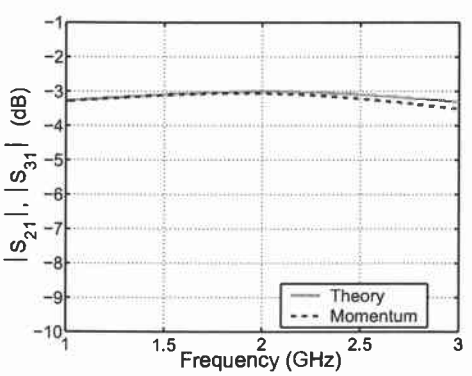

(c)

FIGURE 4.9. Response of the two-conductor-level 3 dB power divider with two cascaded C-section.

TABLE 4.7. Physical geometry of a two conductor level 3 dB power divider using two cascaded C-sections after tuning ($\epsilon_r = 2.2$ and $f_c = 2$ GHz)

Width or Length	Unit (mil)
W_0	42.9
W_1	23.2
W_2	21.12
S_1	50.0
S_2	20.0
L	287.1
b (ground spacing)	60

conductor-level 3 dB power divider with two cascaded C-sections is shown in Figure 4.6(d). The new compact 3 dB power divider design has a significantly reduced footprint size compared to the conventional layout with a footprint reduction of about 83%. The dimensions of the power divider are also well distributed in the different directions.

4.6. Conclusion

In this chapter, a new design methodology for compact RF 3 dB power dividers using folded-line structures in single- and multi-layer configuration has been described. Simple closed-form design equations have been developed and several design examples have been presented. The layout comparison of the new compact 3 dB power divider designs with the folded-line structures (C-sections) shows a significant reduction in footprint size. As seen in the presented design examples, the

new compact power divider designs with a single C-section, two cascaded C-sections, and two cascaded C-sections in two-conductor-level configuration have achieved a size reduction of 67%, 64%, and 83% respectively. Simulation results validated the proposed design methodology.

5. EXPERIMENT

5.1. Fabrication and Measurement of Single Level 3dB Power Divider

To further validate and demonstrate the feasibility of the proposed methodology, the design example of the single-level 3 dB power divider using two cascaded C-sections described in Chapter Four is considered. The physical geometry of the power divider was taken from Table 4.5. The new compact 3 dB Wilkinson power divider was fabricated using RT-5880 Duroid substrate with $\epsilon_r = 2.2$ and ground plane spacing $b = 62$ *mil*. Two 31 *mil* layers are used as top and bottom layers, and they are tightened together after soldering the isolation resistor in the middle. RT-5880 Duroid substrate has a constant and uniform dielectric constant over a wide frequency range with good chemical resistance [1].

The size of the isolation resistor is also taken into account, since it directly affects the layout of the power divider. The chip resistor size is chosen as size code 0603, which corresponds to dimensions 1.6 *mm*, 0.8 *mm*, and 0.45 *mm* for length, width, and thickness, respectively. A smaller resistor size will have less effect on the stripline configuration in the middle of the substrate, when the top and bottom layers are tightened together. However, it will be more difficult to implement the precise location of the circuit. The existence and location of this isolation resistor limits the layout. The resistor has to be on the top layer for surface mounting, unless the resistor can be integrated into the substrate. A photograph of the fabricated 3dB power divider using two cascaded C-sections is shown in Fig. 5.1.

The fabricated compact 3 dB power divider is tested and measured on an HP8722 vector network analyzer. Figure 5.2 shows the response using the present design and the measured data as well as the results from Momentum. The measured response is found to be in good agreement with the proposed theory.

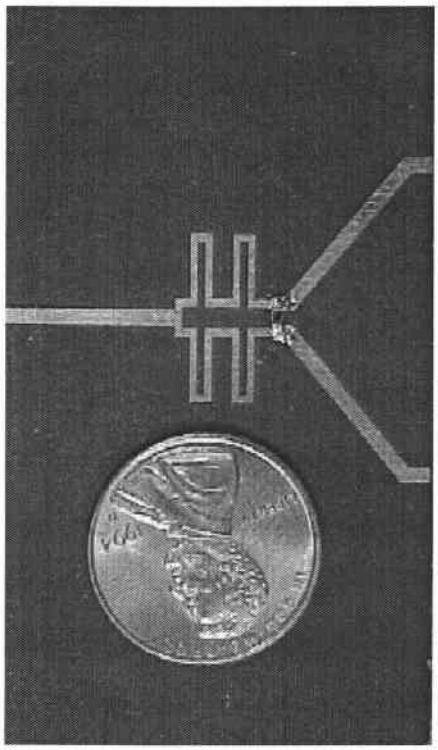

FIGURE 5.1. Photograph of fabricated 3 dB Wilkinson power divider with two cascaded C-sections.

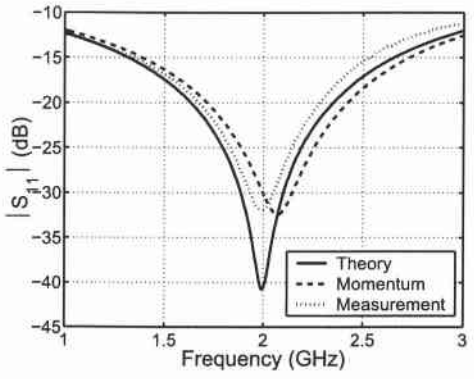

(a)

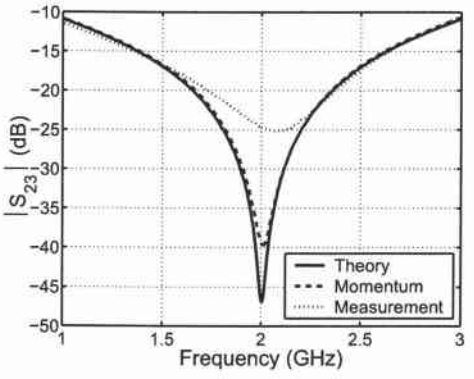

(b)

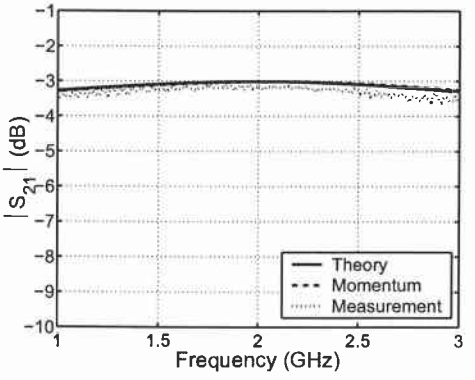

(c)

FIGURE 5.2. Computed and measured S-parameters for a 3dB power divider using two cascaded C-sections in a single conductor level.

5.2. Discussion

The electrical characteristics of the fabricated power divider are mainly determined by the physical geometry of the stripline configuration. During the process of fabrication, many of the physical parameters may be inaccurate. Thus, a sensitivity analysis on several design parameters such as the conductor width W, the spacing of the coupled lines S, and the height of dielectic layer h is needed to observe the tolerance of the designed power divider performance [24]. Knowing the sensitivity to each parameter can provide a worst case error estimate by summing up the maximum deviation for each parameter. Since the most important and complicated parts in the power divider design are the C-sections, the sensitivity to W and S as well as h in the C-sections is evaluated.

Figure 5.3 shows the sensitivity to conductor width in the reflection coefficient (S_{11}) at the input port and the isolation between two output ports (S_{23}). A 5% deviation in conductor width causes an increase in the minimum of S_{11} from about -88 dB to over -32 dB, and an increase in the minimum of S_{23} from about -56 dB to over -39 dB. A 10% deviation in conductor width leads to an increase in minimum of S_{11} to about -25 dB and of minimum S_{23} to about -32 dB.

The sensitivity of the reflection at the input port and the isolation between the two output ports to spacing of the coupled lines (C-section) is shown in Figure 5.4. A 5% deviation in spacing of the coupled lines can lead to about 32 dB difference in $|S_{11}|$ and 3 dB difference in $|S_{23}|$. A 10% deviation in spacing of the coupled lines can conduce to about 37 dB difference in S_{11} and 6 dB difference in S_{23}. The resonant frequency shifts to lower frequency direction by about 0.5% for $|S_{11}|$ and 1% for $|S_{23}|$ for every 5% increment in spacing of the coupled lines.

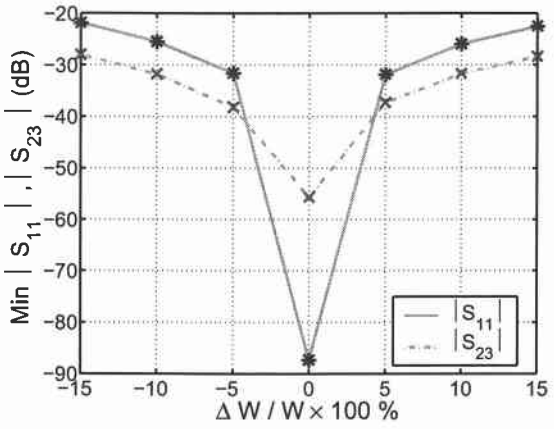

(a)

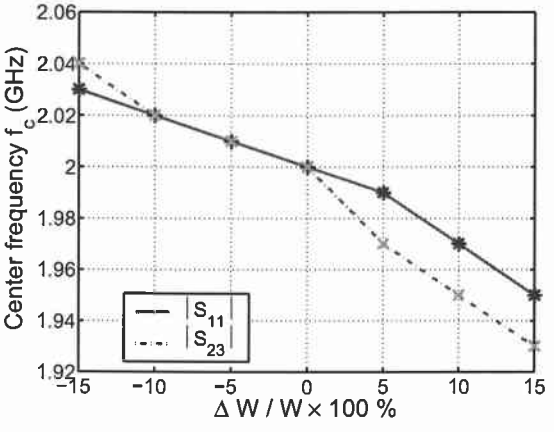

(b)

FIGURE 5.3. Sensitivity to conductor width W in C-section of (a) $| s_{11} |$ and $| s_{23} |$, (b) f_c

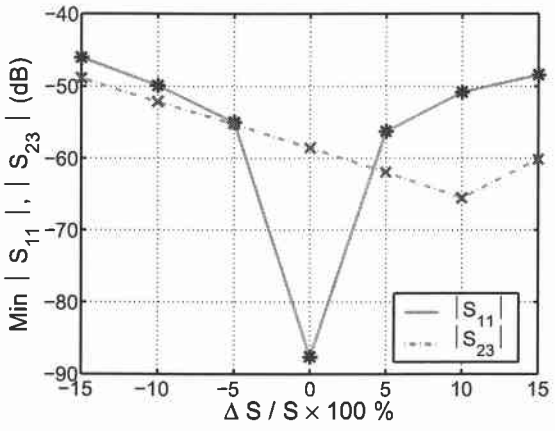

(a)

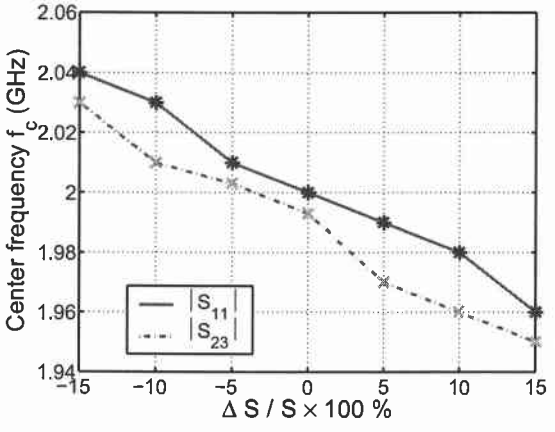

(b)

FIGURE 5.4. Sensitivity to spacing S in C-section of (a) $\mid s_{11} \mid$ and $\mid s_{23} \mid$, (b) f_c

The sensitivity to dielectric height of the reflection at the input port and the isolation between two output ports is shown in Figure 5.5. A 5% deviation of the dielectric height will cause about a 49 dB increase in $|S_{11}|$ and a 15 dB increase in $|S_{23}|$. A 10% deviation of the dielectric height can lead to about 55 dB increase in S_{11} and 19 dB increase in S_{23}. The resonant frequency shifts to higher frequency direction by about 1% for every 5% increment in spacing of the coupled lines.

5.3. Conclusion

In this Chapter, experimental validation for the design example of the single-level 3 dB power divider using two cascaded C-sections is presented. The fabrication procedure of the power divider is discussed. The measured response is in good agreement compared with the simulation results. To observe the tolerance of the power divider performance, a simple sensitivity analysis for conductor width, spacing of the coupled lines, and dielectric height of the C-section was performed.

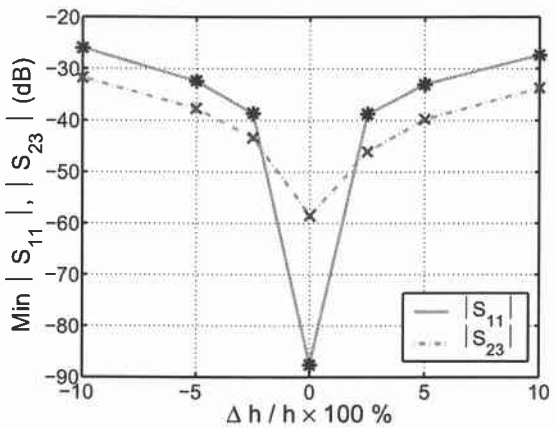

(a)

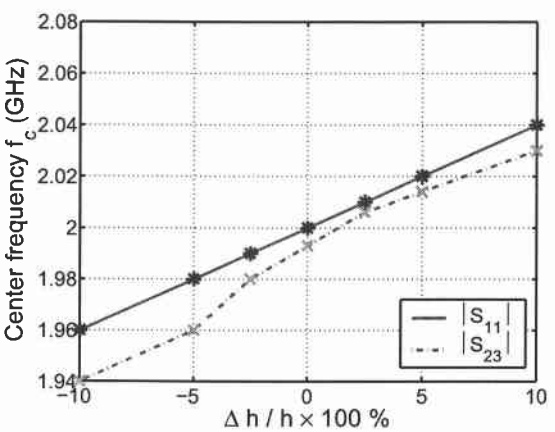

(b)

FIGURE 5.5. Sensitivity to dielectric height h of (a) $\mid s_{11} \mid$ and $\mid s_{23} \mid$, (b) f_c

6. CONCLUSION

This thesis presented a new methodology for the design of compact folded-line RF power dividers in single- and multi-level configurations. In Chapter Two, conventional power dividers such as the lossless T-junction, resistive T-junction, and Wilkinson power dividers were reviewed and their characteristics were analyzed. The conventional Wilkinson power divider offers the attractive properties of ideally having all output ports matched as well as having perfect isolation between the two output ports. For RF applications, however, the conventional design results in a large footprint area due to the large physical length of the quarter-wavelength sections. This motivated the design of new compact configurations by reducing the physical size of the quarter-wavelength sections in the conventional design. Chapter Three introduced the concept of folded lines to reduce the physical size of a quarter-wavelength section. The folded lines can be modeled as uniform coupled lines with appropriate interconnections at the ends. This formulation enabled the use of a simple network representation for the coupled-line sections. In particular, a single C-section consisting of one fold and two coupled lines was considered as a basic building block, and design equations were formulated. In Chapter Four, a new design methodology for compact 3 dB RF power dividers using the folded-line concept in single- and multi-layer configurations was introduced, and design examples were presented. Simple closed-form design equations for the power divider with a single C-section and two cascaded C-section were developed. Significant size reductions in footprint area of the proposed power dividers between 67% and 83% of the conventional design were achieved. Chapter Five presented the measured response of a compact 3dB power divider with two cascaded C-sections. The measured results compared well with full-wave electromagnetic simulation results and the theoretical

response. The sensitivity of the power divider performance to fabrication tolerances was also studied by varying several physical parameters.

In addition to the design of compact RF power dividers, the techniques discussed in this thesis are applicable to various other compact embedded passive components using quarter-wavelength line segments including baluns and couplers. It has been shown that folded lines in single- and multi-conductor level configurations can offer a significant size reduction in footprint area by taking advantage of the 3-D environment. A further reduction in footprint area can be achieved, if the quarter-wavelength sections are folded more tightly in the single- or multi-level configurations resulting in a multiple coupled-line problem, which cannot be accurately represented in terms of cascaded C-sections.

Future work in this area should include the development of new compact topologies and design methodologies for various RF passive components in inhomogeneous environments such as microstrip. Loss effects in the substrate should also be included. A further application of the compact modeling methodology is to passives integrated on chip at microwave frequencies. In the on-chip environment, however, conductor loss effects due the small cross sections of the transmission lines need to be included in the modeling approach.

BIBLIOGRAPHY

[1] RT Duroid 5880 - Rogers Corporation, Rogers, CT.

[2] R. D. Lutz, A. Tripathi, Y. Seo, V. K. Tripathi, "Design Considerations for Embedded Passives," *Wireless Communications Conference*, pp. 181-186, Aug. 1997.

[3] C. Cho, K. C. Gupta, "Design of multilayer coupled line filter circuits," *IEEE MTT-S International Microwave Symposium*, Denver, CO, June. 1997.

[4] V. K. Tripathi *et al.*, "Analysis and Design of Branch-Line Hybrids with coupled lines," *IEEE Trans. Microwave Theory Tech.*, pp. 427-432, Vol. 32, Apr. 1984.

[5] K. Takahashi, M. Sagawa and M. Makimoto, "Miniaturized Hair-pin Resonator Filters and Their Applications to Receiver Front-End MICs," *IEEE MTT-S International Microwave Symposium Digest*, pp. 667-670, Vol. 89.2, 1989.

[6] M. Hirano, K. Nishikawa, I. Toyoda and K. Yamasaki, "Three-Dimensional Passive Circuit Technology for Ultra-Compact MMICs," *IEEE MTT-S International Microwave Symposium Digest*, pp. 1447-1450, Vol. 95.3, 1995.

[7] B. Bhat, S. K. Koul, *Stripline like transmission lines for Microwave Integrated Circuits*, New York, NY: John Wiley & Sons, 1989.

[8] E. Wilkinson, "An N-way hybrid power divider," *IRE Trans. on Microwave Theory and Techniques*, pp. 116-118, vol. MTT-8, Jan. 1960.

[9] David. M. Pozar, *Microwave Engineering 2nd ed*, New York, NY: John Wiley & Sons, 1998.

[10] Raghu K. Settaluri, A. Weisshaar, C. Lim and V. K. Tripathi, "Design of compact multi-level folded-line RF couplers," *IEEE Trans. Microwave Theory Tech.*, pp. 2331-2339, Vol. 47, Dec. 1999.

[11] R. K. Settaluri, G. Sundberg, A. Weisshaar, and V. K. Tripathi, "Compact folded line rat-race hybrid couplers," *Microwave and Guided Wave Letters*, pp. 61-63, Vol. 10, Feb. 2000.

[12] R. K. Settaluri, A. Weisshaar, and V. K. Tripathi, "Compact multi-level folded-line bandpass filters," *IEEE MTT-S International Microwave Symposium Digest*, pp. 311–314, June 2000.

[13] Advanced Design System - Momentum, Agilent Technonolgy, Santa Rosa, CA.

[14] D. Maurin and K. Wu, "A Compact 1.7-2.1 GHz Three-Way Power Combiner using Micostrip Technology with Better than 93.8 % Combining Efficiency," *Microwave and Guided Wave Letters*, pp. 106-108, Vol. 6, Feb. 1996.

[15] J. Reed and G. J. Wheeler, "A method of analysis of symmetrical four-port networks," *IRE Trans. Microwave Theory and Techniques*, Vol. MTT-4, pp. 246-252, Oct. 1956.

[16] V. K. Tripathi, "On the analysis of symmetrical three-line microstrip circuits," *IEEE Trans. Microwave Theory Tech.*, pp. 726-729, Vol. 25, Sept. 1977.

[17] K. D. Marx and R. I. Eastin, "A configuration-oriented SPICE model for multiconductor transmission lines with homogeneous dielectrics," *IEEE Trans. Microwave Theory Tech.*, pp. 1123-1129, Vol. 38, Aug. 1990.

[18] F. Olyslager, N. Fache and D. De Zutter, "New fast and accurate line parameter calculation of general multiconductor transmission lines in multilayerd media," *IEEE Trans. Microwave Theory Tech.*, pp. 901-909, Vol. 39, Jun. 1991.

[19] S. S. Bedair, "Characteristics of some asymmetrical coupled transmission lines," *IEEE Trans. Microwave Theory Tech.*, pp. 108-110, Vol. 38, Jan. 1984.

[20] H. Howe, Jr., *Stripline Circuit Design*, Dedham, MA: Artech Hose, 1974.

[21] Advanced Design System - Agilent Technology, Santa Rosa, CA.

[22] C. Lim, Raghu K. Settaluri, V. K. Tripathi and A. Weisshaar , "Compact folded-line RF power dividers," *Proc 34th Int Symp Microelectronics*(IMAPS'2001), pp. 725-730, Vol. 47, Dec. 2001.

[23] C. Lim, Raghu K. Settaluri, V. K. Tripathi and A. Weisshaar, "Compact single-level and multilevel folded-line RF power dividers," *Microwave and Optical Technology Letters*, pp. 187-189, Vol. 39, Nov. 2003.

[24] S. D. Shamasundara and K.C. Gupta, "Sensitivity Analysis of Coupled Microstrip Directional Couplers," *IEEE Trans. Microwave Theory Tech.*, pp. 108-110, Vol. 26, Oct. 1978.